Journal of
Ceramic Science
and Technology

J. Ceram. Sci. Tech., **05** [03] 193-198 (2014)
DOI: 10.4416/JCST2014-00002
available online at: http://www.ceramic-science.com

Effect of Alkali Concentration and Reaction Time on the Morphology of ZnO Nano-Microparticles Prepared by Hydrothermal Method

A. M. EL-Rafei and M. F. Zawrah*

National Research Center, Refractories, Ceramics and Building
Material Department, 12622-Dokki, Cairo, Egypt.

received February 03, 2014; received in revised form April 09, 2014; accepted May 05, 2014

Abstract

A low-temperature hydrothermal method was used to prepare ZnO nano-microparticles using surfactant-free solutions. The effect of the alkali concentration (Zn^{2+}/OH^- = 1:1, 1:2, 1:4 and 1:8) and reaction time (1, 2 and 3 hours) on the morphology of the ZnO was studied. The structure and the morphology of the ZnO obtained were investigated by means of XRD and SEM techniques, respectively. The results revealed that the solution basicity and reaction time were important factors affecting the morphology. With an increase in the reaction time, the crystallinity of the phases formed was enhanced. At a low alkali concentration, i.e. 1:1, a ZnO hexagonal prism-like structure with a crystal size of 300 nm – 1.5 μm and $Zn(OH)_2$ amorphous phase were formed. With a further increase to Zn^{2+}/OH^- =1:2, some nanorods and flakes appeared beside the ZnO nanoparticles. When the ratio reached Zn^{2+}/OH^- = 1:4, different morphologies such as nanorods, slices and nanoflakes were obtained. At Zn^{2+}/OH^- = 1:8, the morphology changed into microflowers as the major structure with some nanoparticles and nanosheets as the minor structure.

Keywords: Chemical synthesis, ZnO, nanostructures, x-ray diffraction, SEM

I. Introduction

Nanocrystalline metal oxides play a very important role in many areas of chemistry, physics and materials science. They can adopt a vast number of structural geometries with an electronic structure that can exhibit metallic, semiconductor or insulator characteristics [1].

Zinc oxide (ZnO) is an exceptionally important intrinsic semiconductor with a wide direct band gap of 3.37 e.V. and large excitation binding energy of 60 meV at room temperature. Zinc oxide is already widely used in piezoelectric transducers [2], gas sensors [3], optical waveguides [4], dye-sensitized solar cells [5], varistors [6] and solar cell windows [7] as well as bulk acoustic wave devices [8]. In recent years, one-dimensional (1D) oxides have attracted considerable interest owing to their distinctive geometry characteristics as well as their novel chemical and physical properties. A variety of morphologies including nanowires [9], nanorods [10], hollow spheres [11], nanoflakes [12], nanowhiskers [13], hexagonal prismatic shapes [14], bi-pyramidal and dumbbell-like shapes [15], nanoribbons [16], and flower-like shapes [17] have been synthesized. These structures are expected to have more potential applications in building functional electronic devices with special architectures and distinctive optoelectronic properties. However, morphological control and crystal evolution of ZnO structures are still difficult to achieve. They are proving a great challenge for material scientists.

The complicated procedures, sophisticated equipment or rigid experimental conditions used in chemical vapor deposition, thermal evaporation and sputtering methods severely restrict their large-scale application in industry. In contrast, preparation of ZnO via wet-chemical routes with easily controlled conditions and lower consumption of energy provide a promising option for mass production of this material. Many methods have been developed to synthesize ZnO nanoparticles, including solution-based techniques such as the sol-gel process [18], the hydrothermal method [19], precipitation [20], the microwave method [21], etc.

Most of the previous systematic chemical syntheses showed that ZnO with different morphologies such as flowers and rods can be obtained by altering the concentration of NaOH. One-dimensional ZnO nanostructures with a high aspect ratio have been successfully synthesized by Chen Liangyuan *et al.* [3] in a low-temperature hydrothermal process at 85 °C for 5 h using SDS as surfactant.

Hydrothermal synthesis is becoming popular for environmental reasons, since water is used as a reaction solvent rather than an organic solvent. This method has been widely used to prepare nanomaterials owing to its simplicity, high efficiency and low cost.

In the work described here, a simple low-temperature (120 °C) and surfactant-free hydrothermal method has been developed to synthesize different morphologies of ZnO in alkaline media, using zinc acetate and NaOH as the reactants. The influence of the reaction time and the alkali concentration on the morphology and composition of the hydrothermal products is investigated.

* Corresponding author: mzawrah@hotmail.com

II. Materials and Experimental Procedures

Zinc acetate (99.99 % trace metals basis) and sodium hydroxide (ACS reagent, ≥ 97.0 %, pellets) from (Sigma-Aldrich) were used as starting materials. For the synthesis of zinc oxide under hydrothermal conditions, 25 ml of zinc acetate solution (0.5 M) was filled into a Teflon vessel. An appropriate amount of NaOH was added into the vessel i.e. 0.49, 0.98, 1.96 and 3.92 g. In the present work, different ratios of starting Zn^{2+}/OH^- i.e. 1:1, 1:2, 1:4 and 1:8, were used in preparation of the ZnO. After it had been sealed, the autoclave was treated at 120 °C for 1, 2 and 3 h and then cooled down. After the vessel had been cooled to room temperature, the powders were collected and washed with distilled water several times by means of centrifugation. The powders were then dried in an oven at 100 °C.

The qualitative phase composition of the prepared ZnO was examined with X-ray diffraction (XRD). A Bruker D8 Advance diffractometer with a Cu-Kα target and secondary monochromator (Kv = 40 and mA = 40) was used. The morphology and particle sizes of the as-prepared powders were tested with a high-resolution scanning electron microscope, model Philips XL 30, with accelerating voltage 30 kv.

III. Results and Discussion

Fig. 1 shows the X-ray diffraction patterns of as-prepared ZnO powder at 120 °C for 1, 2 and 3 h using 0.49 g NaOH (i.e. Zn^{2+}/OH^- = 1:1) by the hydrothermal method. As indicated in these patterns, the sample obtained at 1, 2 and 3 h exhibits a wurtzite ZnO structure according to JCPDS 36 – 1451. The following XRD peaks were detected; i.e. (100), (002), (101), (102), (110), (103), (200), (112), (201), (004), (202) at 2θ = 31.8, 34.5, 36.3, 47.6, 56.6, 62.9, 66.3, 68.0, 69.2, 72.5, 76.9, respectively. Also, it is observed that the peak intensities of the ZnO phase increased with increasing reaction time.

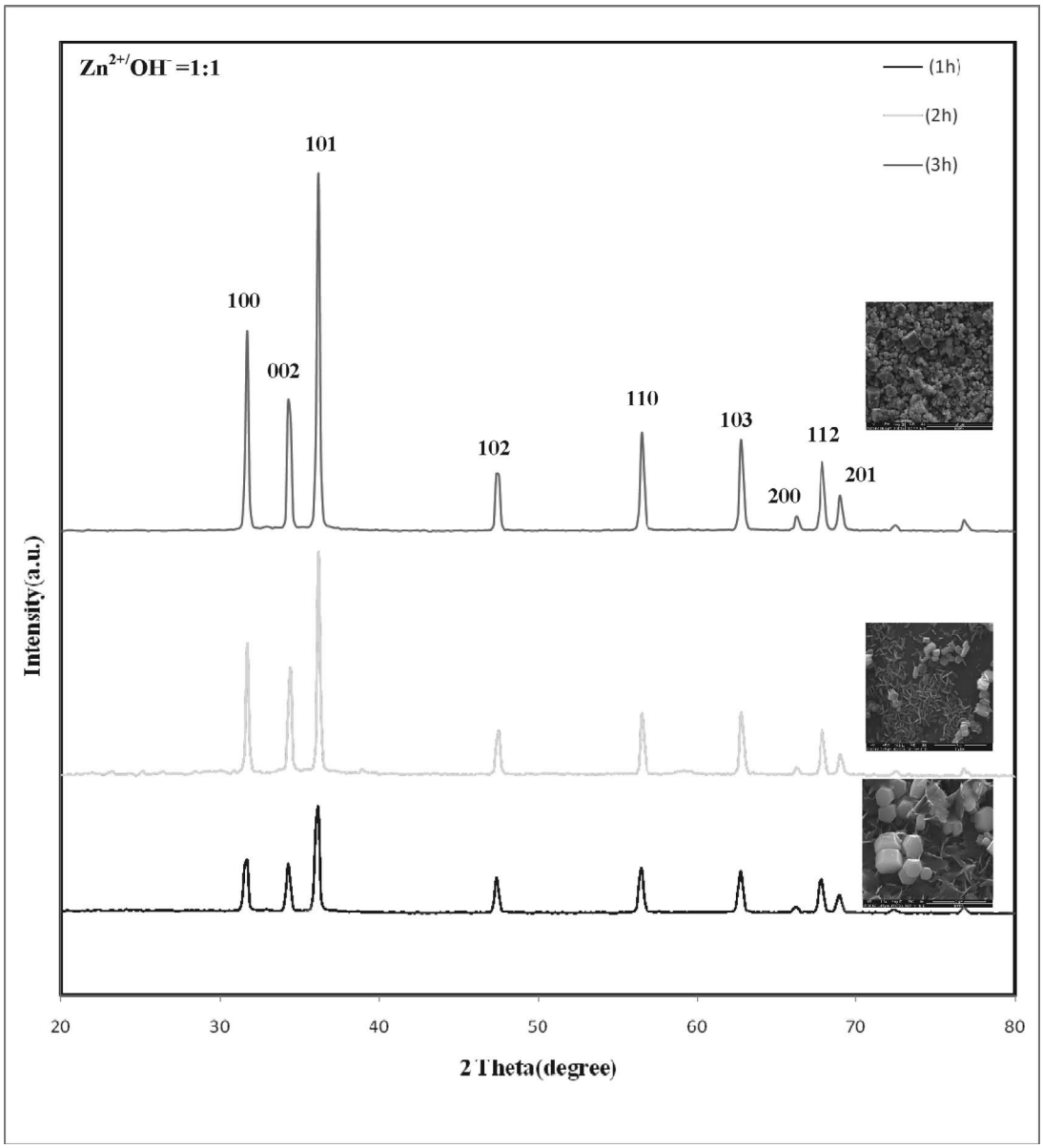

Fig. 1: XRD patterns of the as-prepared ZnO powders using 0.49 g NaOH at 1 h, 2 h and 3 h.

Fig. 2 shows the X-ray diffraction patterns of as-prepared ZnO powder at 120 °C for 1, 2 and 3 h using 0.98 g NaOH (i.e. Zn^{2+}/OH^{-} = 1:2) by the hydrothermal method. It appears that all diffraction peaks for all samples are quite similar to the wurtzite ZnO. It seems that the diffraction peak intensities of ZnO phase increase as the time of the reaction increases. It is worth mentioning that the results of the diffraction patterns of ZnO prepared using 1:4 and 1:8 Zn^{2+}/OH^{-} are very similar to that of ZnO prepared using 1:2 Zn^{+}/OH^{-}.

Figs. 3a-d show SEM images of the as-prepared ZnO obtained at 120 °C for 1 h using different ratios of Zn^{2+}/OH^{-}, i.e. 1:1, 1:2, 1:4 and 1:8, respectively. It is evident that the sample prepared using 0.49 g NaOH (i.e. Zn^{2+}/OH^{-} = 1:1) exhibited a hexagonal prism-like structure of ZnO crystalline phase (Fig. 3a) with crystallite size ranging between 300 nm and 1.5 μm. The apparent amorphous phase is assigned to $Zn(OH)_2$. With a further increase in the NaOH concentration, i.e. Zn^{2+}/OH^{-} =1:2, some nanorods and flakes started to appear (Fig. 3b) beside the ZnO nanoparticles. When the concentration of NaOH reached 1.96 g i.e. Zn^{2+}/OH^{-} = 1:4, different morphologies like nanorods, slices and nanoflakes were obtained (Fig. 3c). With 1.96 g NaOH i.e. Zn^{2+}/OH^{-} = 1:8, the morphology of the obtained ZnO changed into microflowers as the major structure and some nanoparticles and nanosheets as the minor structure (Fig. 3d). The flower-like microstructure with an average size of 10 μm is constructed from many sword-like nanorods.

The higher magnification image of a single flower in Fig. 3e clearly shows that the ZnO rods have a sharp tip radially aligned from the center. The microstructure of individual microflower is composed of many sword-like nanorods with a diameter of 50 – 230 nm, a length of 1 – 1.5 μm and a sharp tip. This well-defined microstructure is similar to that prepared by Xie *et al.* 22, who prepared ZnO flowers composed of sharp-tipped ZnO rods at Zn^{2+}:OH^{-} = 1:4 and 1:5. Wang *et al.* [15] also prepared ZnO flowers with the hydrothermal method at 90 °C for 5 h with an average diameter of 5 – 6 μm.

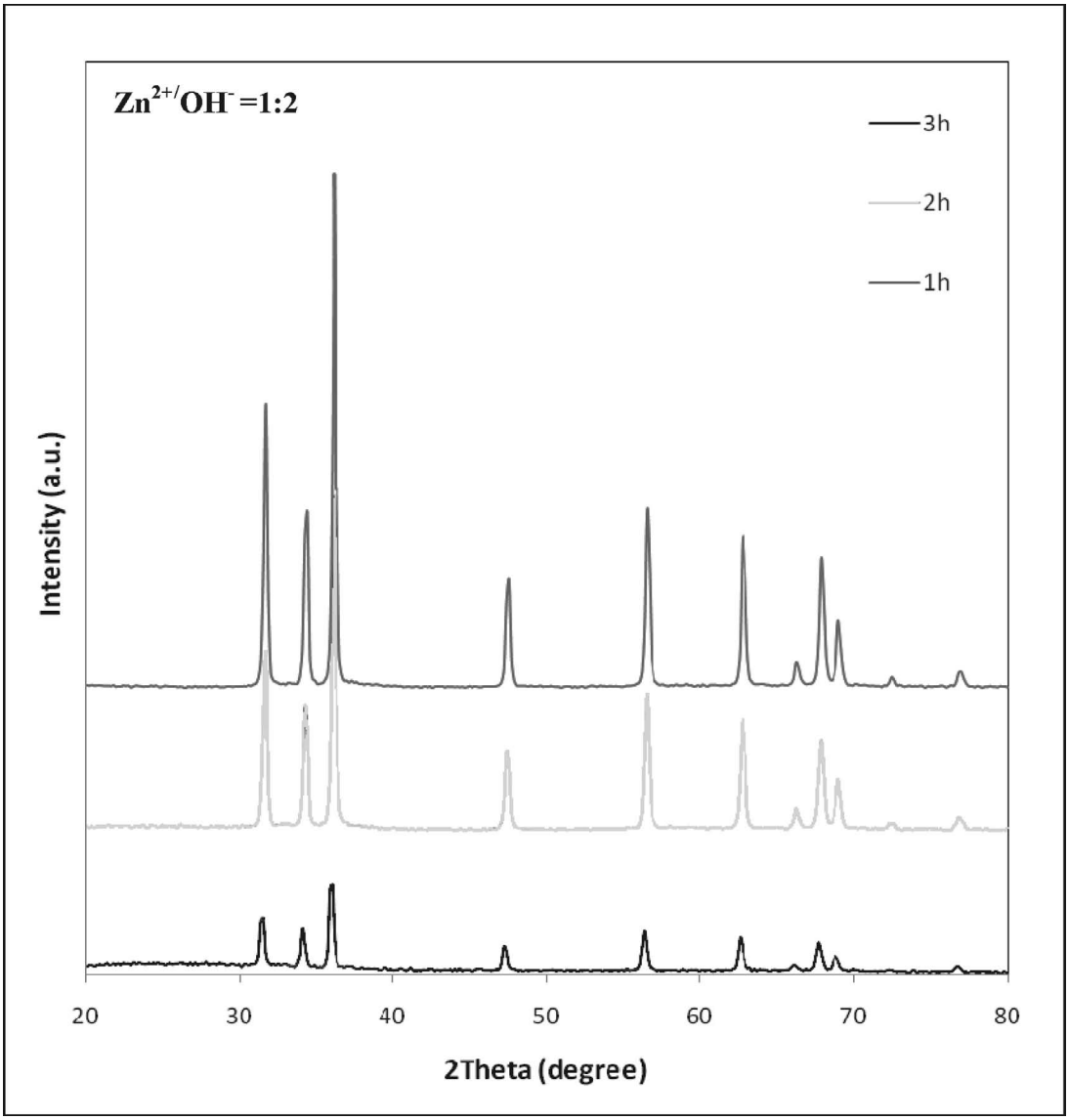

Fig. 2: XRD patterns of the as-prepared ZnO powders using 0.98 g NaOH at 1 h, 2 h and 3 h.

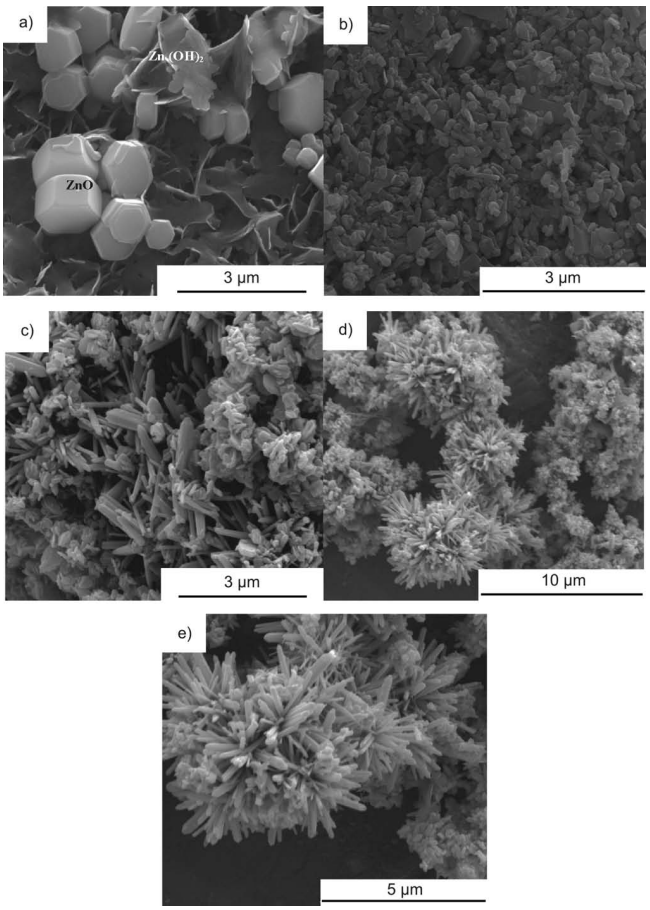

Fig. 3 : SEM images of as-prepared samples obtained at 120 °C for 1 h using different ratios of (a) Zn^{2+}:OH^- = 1:1, (b) 1:2, (c) 1:4, (d) 1:8, (e) high-magnification SEM image of the ZnO flowers.

As the duration of the hydrothermal reaction increases to 2 h (Fig. 4), the crystallinity of the ZnO increases and the prepared powder retains its microstructure architecture with larger grain sizes for all NaOH concentrations. For the ZnO prepared using 1:1 Zn^+/OH^- (Fig. 4a), the nucleation of hexagonal disks of ZnO crystals increased at the expense of $Zn(OH)_2$. For Zn^+/OH^- = 1:2, the nanorods are longer as a result of growth along (002) direction. For Zn^+/OH^- = 1:4, the crystal growth of ZnO nanorods is somewhat suppressed along the (002) direction, resulting in nanoslices and nanoflakes. Thruster vanes started to appear beside other morphologies like nanorods, slices and nanoflakes. For the highest concentration of NaOH (Zn^+/OH^- = 1:8), the formed microflower composed of nanorods became thicker and longer. In the present work, we succeeded in preparing a ZnO microflower at a relatively low temperature compared with the finding of G. Nagaraju [23] who prepared a star-like structure at 180 °C for 6 h. A further increase in the treatment time to 3 h has no effect on the crystal shape of ZnO for all concentrations of NaOH as shown in Fig. 5, except there are an enhancement of crystal size and Zn(OH)2 disappeared completely. The only difference is the enhancement of crystal size. Samaele *et al.* [24] claimed that the precipitation of ZnO particles has been usually described through a growth unit that might be either $Zn(OH)_2$ or $Zn(OH)_4^{2-}$ ions, depending on the pH, temperature and synthetic methods. Xie *et al.* [22] proposed that ZnO can grow by the $Zn(OH)_2 - Zn(OH)_4^{2-}$ species when the mole ratio of Zn^{2+}:OH^- is within a range of 1:4 – 1:7. However, $Zn(OH)_4^{2-}$ ions are the precursors of Zn^{2+}:OH^- in the range of 1:8 – 1:9.

The formation process of ZnO nano- and microparticles can be discussed as follows; it is well accepted that crystal formation in solution can be divided into two stages: crystal nucleation followed by crystal growth for the crystal nuclei. The obtained particle size and shape depend on the nucleation rate as well as the crystal growth rate. At the lowest concentration of NaOH, i.e. Zn+/OH- = 1:1, the rate of formation of the ZnO nucleus is very slow as indicated by the presence of amorphous $Zn(OH)_2$ in the SEM for the reaction time of 1 h. This means that the rate of the transformation of $Zn(OH)_2$ into hexagonal prism ZnO is low and increases with an increase in the basicity of solution and time of the reaction according to the following dissolution-reprecipitation mechanism:

$$2Zn_{aq}^{+2} + 2OH^- \rightarrow 2Zn(OH)_2(s) \quad (1)$$

$$Zn(OH)_2 \rightarrow ZnO(s)(\text{nucleation}) \quad (2)$$

For needle-like ZnO, the nucleation and growth rates of the ZnO crystal are relatively slow. Therefore, a suitable amount of ZnO nuclei generates in the initial stage of the aging step. After that, appropriate number of growth units is preferentially supplied for the c-axis direction for every nucleus to form ZnO nanorods as seen in the Fig. 3b. As the basicity of the solution increases, the crystal growth along the [0 0 2] direction is suppressed. Nanoslices can be obtained owing to quasi 1D growth, clearly observed in Fig. 3c. Finally, when multiple nanoslices grow further, nanothruster vanes can be formed by self-assembled growth as shown in Fig. 5c.

For the reactions of flower-like ZnO formation, ZnO nuclei formed spontaneously from the dehydration of abundant $Zn(OH)_4^{2-}$ ions and followed by crystal growth. During the latter process, growth unit $Zn(OH)_4^{2-}$ is directly incorporated into ZnO crystallites under given conditions, according to the following reaction:

$$Zn^2(aq) + 2OH^- \rightarrow Zn(OH)_2(s) \quad (3)$$

$$Zn(OH)_2 + 2OH^- \rightarrow [Zn(OH)_4]^{2-}(aq) \quad (4)$$

$$Zn^{2+} + 4OH^- \rightarrow [Zn(OH)_4]^{2-}(aq) \quad (5)$$

$$[Zn(OH)_4]^{2-} \rightarrow ZnO(s) + H_2O + 2OH^-(\text{nucleation}) \quad (6)$$

Both nucleation and crystal growth are very fast. At the beginning of the aging step, large amounts of ZnO nuclei form, and owing to the driving forces of high surface energy and electrostatic force, some ZnO nuclei easily aggregate together immediately [22, 25] then each nucleus in the aggregate grows anisotropically along its c-axis, resulting in flower-like nanorod-assemblies [26]. This is very similar to our results obtained when Zn^{2+}:OH^- is 1:8.

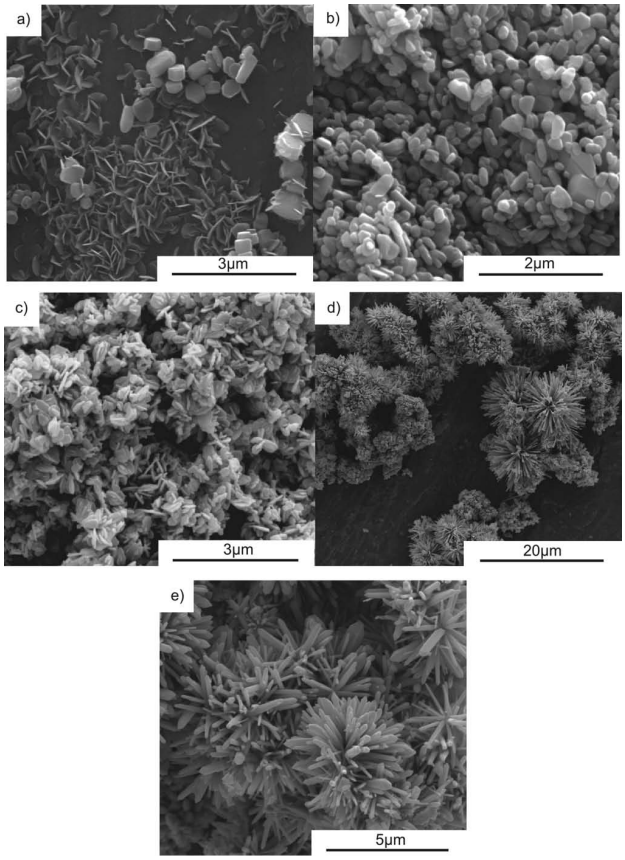

Fig. 4: SEM images of as-prepared samples obtained at 120 °C for 2 h using different ratios of (a) Zn^{2+}:OH^- = 1:1, (b) 1:2, (c) 1:4, (d) 1:8, (e) high-magnification SEM image of the ZnO flowers.

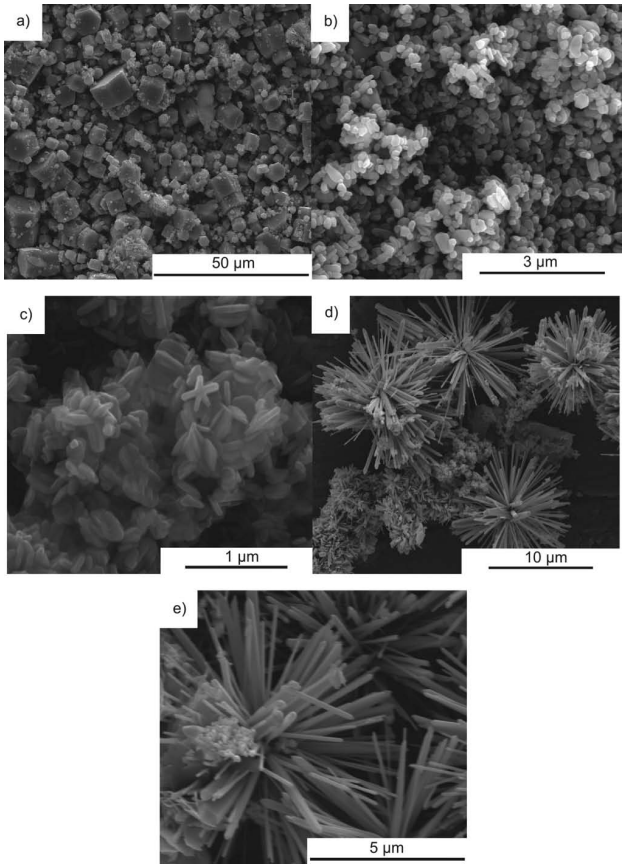

Fig. 5: SEM images of as-prepared samples obtained at 120 °C for 3 h using different ratios of (a) Zn^{2+}:OH^- = 1:1, (b) 1:2, (c) 1:4, (d) 1:8, (e) high-magnification SEM image of the ZnO flowers.

It was well established that the growth mechanism of ZnO crystals involves the formation of growth units along the c-axis based on a dehydration reaction because of the very low surface energy of the (0001) facet [27–28]. The crystal growth is initiated preferentially from the most thermodynamically active clusters on the surface [29]. In the solution method, the velocity of crystal growth in different directions has been reported to be: V(0001) >V(1011) > V(1010) >V(1011) >V(0001) [30]. Therefore, the (0001) plane is the most rapid growth plane so its disappearance is quicker in the hydrothermal process, which leads finally to hexagonal nanorods. Such hexagonal morphology is consistent with the idealized growth behavior of the ZnO crystal described by Laudise and Ballman [31], who deemed that ZnO prefers to grow along the [0001] direction. The crystal facet with faster growth velocity tends to disappear while the facet with slower growth velocity tends to remain [32].

IV. Conclusions

Different morphologies of ZnO nano-microparticles have been prepared at 120 °C for 1–3 hours by means of the hydrothermal method. This method requires a relatively low temperature and short time compared with either the same synthetic or other techniques. The solution basicity and reaction time were important factors affecting the morphology of the final product. With an increase in the reaction time, the crystallinity of the phases formed was enhanced. When the alkali concentration was changed, different morphologies of ZnO were obtained.

References

1 Fernández-Garcia, M., Martínez-Arias, A., Hanson, J.C., Rodriguez, J.A.: Nanostructured oxides in Chemistry: Characterization and properties, *Chem. Rev.*, **104**, 4063–4104, (2004).

2 Xian Gao, P., Wang, Z.L.: Nanoarchitectures of semiconducting and piezoelectric zinc oxide, *J. Appl. Phys.*, **97**, (2005).

3 Liangyuan, C., Zhiyong, L., Shouli, B., Kewei, Z., Dianqing, L., Aifan, C., Liu, C.C.: Synthesis of 1-dimensional ZnO and its sensing property for CO, *Sensor. Actuat. B*, **143**, 620–628, (2010).

4 Struk, P., Pustelny, T., Gut, K., Gołaszewska, K., Kaminska, E., Ekielski, M., Pasternak, I., Łusakowska, E., Piotrowska, A.: Planar optical waveguides based on thin ZnO layers, *Acta Phys. Pol. A.*, **116**, (2009).

5 Law, M., Greene, L.E., Johnson, J.C., Saykally, R., Yang, P.D.: Nanowire dye-sensitized solar cells, *Nat. Mater.*, **4**, 455–459, (2005).

6 Kanai, H., Imai, M., Takahashi, T.: A high-resolution transmission electron microscope study of a zinc oxide varistor, *J. Mater. Sci.,* **20**, 3957–3966, (1985).

7 Fuhs, W.: ZnO window layers for solar cells, N.H. Nickel and E. Terukov (eds.), Zinc Oxide – A material for micro- and optoelectronic applications, 2005 Springer. 197–209

8 Ferblantier, G., Mailly, F., Al Asmar, R., Foucaran, A., Pascal-Delannoy, F.: Deposition of zinc oxide thin films for application in bulk acoustic wave resonator, *Sensor. Actuat.A: Physical*, **122**, [2], (2005).

9 Sun, G., Cao, M., Wang, Y., Hu, C., Liu, Y., Ren, L., Pu, Z.: Anionic surfactant-assisted hydrothermal synthesis of high-aspect-ratio ZnO nanowires and their photoluminescence property, *Mater. Lett.,* **60**, 2777–2782, (2006).

[10] Yin, H., Xu, Z., Wang, G., Bai, J., Bao, H.: Study of assembling ZnO nanorods into chrysanthemum-like crystals, *Mater. Chem. Phys.*, **91**, 130 – 133, (2005).

[11] Tao, J.C., Chen, X., Sun, Y., Shen, Y., Dai, N.: Controllable preparation of ZnO hollow microspheres by self-assembled block copolymer, *Colloid. Surface. A,* **330**, 67 – 71, (2008).

[12] Ni, Y., Wu, G., Zhang, X., Cao, X., Hu, G., Tao, A., Yang, Z., Wei, X.: Hydrothermal preparation, characterization and property research of flowerlike ZnO nanocrystals built up by nanoflakes, *Mater. Res. Bull.*, **43**, 2919 – 2928, (2008).

[13] Li, F., Hu, L., Li, Z., Huang, X.: Influence of temperature on the morphology and luminescence of ZnO micro and nanostructures prepared by CTAB-assisted hydrothermal method, *J. Alloys Compd.*, **465**, L14 – L19, (2008).

[14] Li, P., Wei, Y., Liu, H., Wang, X.K.; Growth of well-defined ZnO microparticles with additives from aqueous solution, *J. Solid State Chem.*, **178**, 855 – 860, (2005).

[15] Wang, B.G., Shi, E.W., Zhong, W.Z.: Twinning morphologies and mechanisms of ZnO crystallites under hydrothermal conditions, *Cryst. Res. Technol.*, **33**, 937 – 941, (1998).

[16] Yan, H., Johnson, J., Law, M., He, R., Knutsen, K., McKinney, J.R., Pham, J., Saykally, R., Yang, P.: ZnO nanoribbon microcavity lasers, *Adv. Mater.*, **15**, 1907 – 1911, (2003).

[17] Liu, J.P., Huang, X.T., Li, Y.Y., Duan, J.X., Ai, H.H.: Large-scale synthesis of flower-like ZnO structures by a surfactant-free and low-temperature process, *Mater. Chem. Phys.*, **98**, 523 – 527, (2006).

[18] Hwang Y.H., Seo, S., Bae, B.: Fabrication and characterization of sol-gel-derived zinc oxide thin-film transistor, *J. Mater. Res.,* **25**, (4), 695 – 700, (2010).

[19] Ni, Y-H., Wei, X.W., Hong, J.M., Ye, Y.: Hydrothermal preparation and optical properties of ZnO nanorods, *Mater. Sci. Eng. B,* **121**, 42 – 47, (2005).

[20] Lanje, A.S., Sharma, S.J., Ningthoujam, R.S., Ahn, J.-S., Pode, R.B.: Low temperature dielectric studies of zinc oxide (ZnO) nanoparticles prepared by precipitation method, *Adv. Powder Technol.*, **24**, 331 – 335, (2013).

[21] Zhu, L., Zheng, Y., Hao, T., Shi, X., Chen, Y., Ou-Yang, J.: Synthesis of hierarchical ZnO nanobelts via Zn(OH)F intermediate using ionic liquid-assistant microwave irradiation method, *Mater. Lett.,* **63**, 2405 – 2408, (2009).

[22] Xie, J., Li, P., Wang. Y., Wei, Y.: Synthesis of needle- and flower-like ZnO microstructures by a simple aqueous solution route, *J. Phys.Chem. Solids,* **70**, 112 – 116, (2009).

[23] Nagaraju, G., Ashoka, S., Chithaiah, P., Tharamani, C.N., Chandrappa, G.T.: Surfactant free hydrothermally derived ZnO nanowires, nanorods, microrods and their characterization, *Mat. Sci. Semicon. Proc.*, **13**, 21 – 28, (2010).

[24] Samaele, N., Amornpitoksuk, P., Suwanboon, S.: Effect of pH on the morphology and optical properties of modified ZnO particles by SDS via a precipitation method, *Powder Technol.*, **203**, 243 – 247, (2010).

[25] Mc Bride, R.A., Kelly, J.M., Mc Cormack, D.E.: Growth of well-defined ZnO microparticles by hydroxide ion hydrolysis of zinc salts, *J. Mater. Chem.,* **13**, 1196 – 1201, (2003).

[26] Xie, J., Li, Y., Zhao, W., Bian, L., Wei, Y.: Simple fabrication and photocatalytic activity of ZnO particles with different morphologies, *Powder Technol.*, **207**, 140 – 144, (2011).

[27] Xu, C.X., Sun, X.W.: Characteristics and growth mechanism of ZnO whiskers fabricated by vapor phase transport, *Jpn. J. Appl. Phys.*, **42**, 4949 – 4952, (2003).

[28] Hu, J.Q., Li, Q., Wong, N.B., Lee, C.S., Lee, S.T.: Synthesis of uniform hexagonal prismatic ZnO whiskers, *Chem. Mater.*, **14**, 1216 – 1219, (2002).

[29] Mo, M.S., Yu, J.C., Zhang, L.Z.: Self-assembly of ZnO nanorods and nanosheets into hollow microhemispheres and microspheres, *Adv. Mater.*, **17**, 756 – 760, (2005).

[30] Li, P., Wei, Y., Liu, H., Wang, X.K.: Growth of well-defined ZnO microparticles with additives from aqueous solution, *J. Solid State Chem.*, **178**, 855 – 860, (2005).

[31] Laudise, R.A., Balmann, A.A.: Hydrothermal synthesis of zinc oxide and zinc sulfide, *J. Phys. Chem.*, **64**, 688 – 691, (1960).

[32] Li, W.J., Shi, E.W., Zhong, W.G., Yin, Z.W.: Growth mechanism and growth habit of oxide crystals, *J. Cryst. Growth,* **203**, 186 – 196, (1999).